5

Fundamental magnetic properties at nanometer scale

Abdulaziz Aiyedh Alharbi

King Abdulaziz City for Science and Technology (KACST), P. O. Box 6086, Riyadh 11442, Saudi Arabia

Outline:

Introduction

The determining physical properties of materials, such as electric, optical and magnetic properties, are important to employ such materials in sufficient way. In the past, we normally take the measurements on enough quantities of the sample and then we assume that the results should be right at any size. In fact, it is proven that the properties of materials have different behaviors at nanoscale, and therefore the size factor can be played an important role in the properties of materials. At this scale, nanomaterials show exceptional properties which can be employed to improve the current materials or create new ones. This is because matter at nano level is dominated by laws of quantum rather than classical mechanics.
The magnetic nanomaterial is an attractive topic for many researchers around the world due to its promising applications such as data storage, field effect transistor and magnetic sensor. In general, the magnetization curve gives information about the magnetic properties of material. If this curve is a straight line shape then the material is known as paramagnetic, however if it is a closed loop shape which is called hysteresis loop then the material is known as ferromagnetic**.** It provides us with very useful information about the magnetic materials and then helps us to employ them in suitable applications. For example, the coercive field (H_c) of hysteresis curve tells us whether this material is a soft or hard magnetic material. For the soft one, the H_c is small and it can be alternating very easy with small magnetic field which makes this material suitable for transformers and electrical machinery. For the hard magnetic, the coercive field is quite big compared with that one in the soft magnetic which can be used in data storage for example.
At nanoscale, the magnetic materials can be tailored to be soft or hard magnetic materials by designing the nanostructure of such materials, leading to improve the properties of magnetic materials and emerging new properties such as super paramagnetic of single magnetic domain.
In this chapter, we will give overview of fundamental magnetic properties at nanometer scale, starting with general synthesis and characterization of nanostructured materials and focusing on nanomagnetic materials by matching them with examples. The significant phenomena of nanomagnetism will be discussed such as magnetoresistance, magnetoimpedence, spin torque transfer and surface effects. Also, multi-layered films and exchange bias with their possible applications, and interface effects challenging will be taken into account. In addition, the growth and protection of magnetic nanoparticles will be considered. Finally, the imaging and characterization of magnetic materials will be discussed at the end of this chapter.

Design, synthesis and characterization of nanostructured materials

There are many ways to fabricate nanostructures material for magnetic application. It is hard to cover all synthesized processes, but in this section, we will present the most common ones by giving the general ideas how it works and the specialty of each method.

The Growth techniques

The growth techniques which will be discussed in this section are Pulsed Laser Deposition (PLD), Sputtering, and Molecular Beam Epitaxy (MBE). The principle of each technique will be considered. Also, the advantages and disadvantages will be taken into account.

Pulsed Laser Deposition (PLD)

The schematic diagram of the PLD system is shown in Figure (5.1). Generally, the system is made of three main components, namely the laser, the optical arrangement and the deposition chamber. Normally, an excimer XeCl laser with 308 nm wavelength is used in the ablation process. It can generate a pulse of energy of up to 400 mJ, with a pulse length of 28 ns operating at a repetition rate of 10Hz. Secondly; the optical system involves a quartz lens that is sited between the laser and the deposition chamber. This lens plays an important role in focusing the laser on the small area of the target (about 3 mm2). The last part of the PLD system is the deposition chamber which is a stainless-steel, high-vacuum compartment. The target and substrate holder are located inside the chamber. The target holder can be rotated during ablation by an electric motor [1].

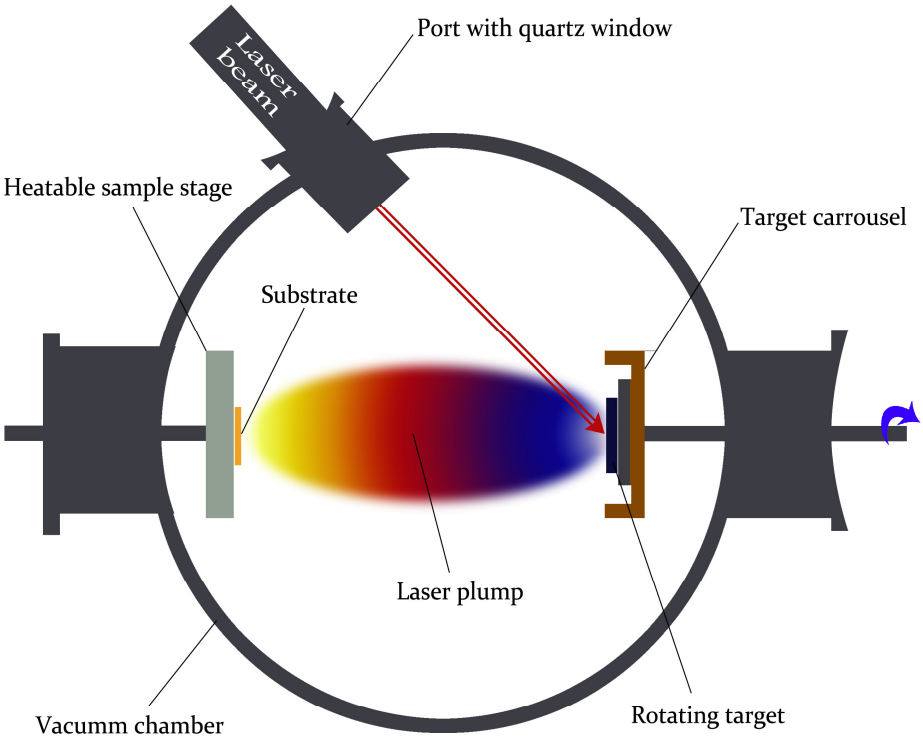

FIGURE 5.1
The schematic diagram of the PLD system

The PLD system has many advantages compared with other techniques. For example, because the laser is separate from the deposition chamber, it is possible to fabricate multilayer films by changing various targets in and out of the beam's focal point which is inside the chamber. Moreover, it can be used to fabricate films at different pressures with a high degree of control even at high pressures. In addition, the PLD technique is considered to be easy and inexpensive. On the other hand, PLD also has drawbacks. One of the most common disadvantages is splashing which

can result in the formation of defects on the substrate. This can affect the quality of films and therefore can affect properties such as electric transport [1,2].

Magnetron Sputtering

Magnetron sputtering is a physical technique which is wildly used for making magnetic thin films. It is more suitable for industry due to its deposition rate which is high enough (around 1 micrometer per min) and also making multilayered film can be achieved by rotating multiple targets [3,4].
We can summarize the procedure of Magnetron sputtering on the following steps as shown in Figure (5.2):

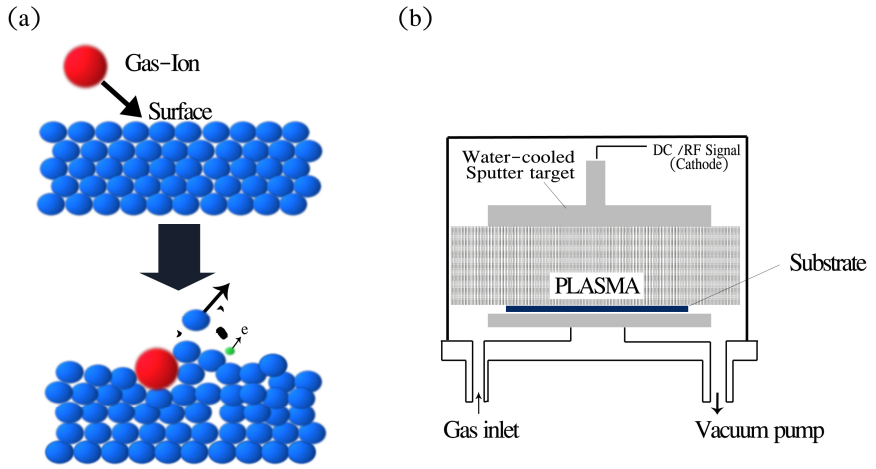

FIGURE 5.2
The schematic diagram of growth procedure of magnetron sputtering system

1. Firstly, creating a plasma inside the chamber (mostly is Argon) by applying of a large potential between two parallel plates, and then the positive ions move to the target which is negative bias.
2. Highly energetic ions hitting the target surface which leads to release individual atoms. A static magnetic field is applied close to the target to confine the plasma to the target area and also to stop secondary electrons which are produced by the target, from impinging on the substrate and result in heating or damaging it.

3. These ejected atoms from the target surface will fly and deposit finally on the substrate.

Sometime, the magnetic poles can be added on substrate holder to align the growth on a specific direction.

Molecular Beam Epitaxy (MBE)

Molecular Beam Epitaxy (MBE) machine is basically an ultra high vacuum (UHV) for fabricating high precision thin film with monolayer control. It is started to use from 1970s to produce high purity

semiconductor films. Later, this technique has became widely use for epitaxial layers even for metals, insulator and superconductor.
The growth principle of MBE is not quite complicated: it consists essentially of material sources, which can be either solid or gaseous. In general, MBE machine has array of multiple sources to allow produce multilayer structure by alternating the materials using shutter. Once the material sources are heated up, the shutter is open for the selected materials to allow the evaporated atoms to deposit on the substrate which is normally made of single crystal. If the required thickness is reached the system close the shutter directly and then open the shutter for the second layer and so on. It is possible to make single atomic layer around 3 Angstroms. Magnetic multilayers for spin valve structure are fabricated using this type of technique [4].

MBE can be combined with a set of in-situ tools such as Reflection High Electron Diffraction (RHEED) which provide us very useful information about the film thickness in particular ultra thin film around 2-3 nm.

The characterization techniques

Scanning Electron Microscopy (SEM)

Scanning electron microscopy (SEM) is a kind of electron microscope that images a sample by scanning it with high energy electron beam. Basically, electron microscopy uses electrons instead of photons which are used in optical microscopy. We can summarize the major difference in the following:

1. The wavelength of accelerated electrons is much smaller than the wavelength of photons and therefore leads to greater resolution.
2. Electrons interact with matter much strongly than photons.
3. Electrons are charged particles and may thus be focused by electric or magnetic field.

SEM is an important tool for material characterization especially for microstructural and morphological properties. SEM can provide important information about the features of surface geometry of an object, such as texture, shape, size and arrangement of the particles laying on the surface of the sample or have been exposed by grinding or chemical etching. Furthermore, it can show the arrangement of atoms in the specimen and their degree of order [5].

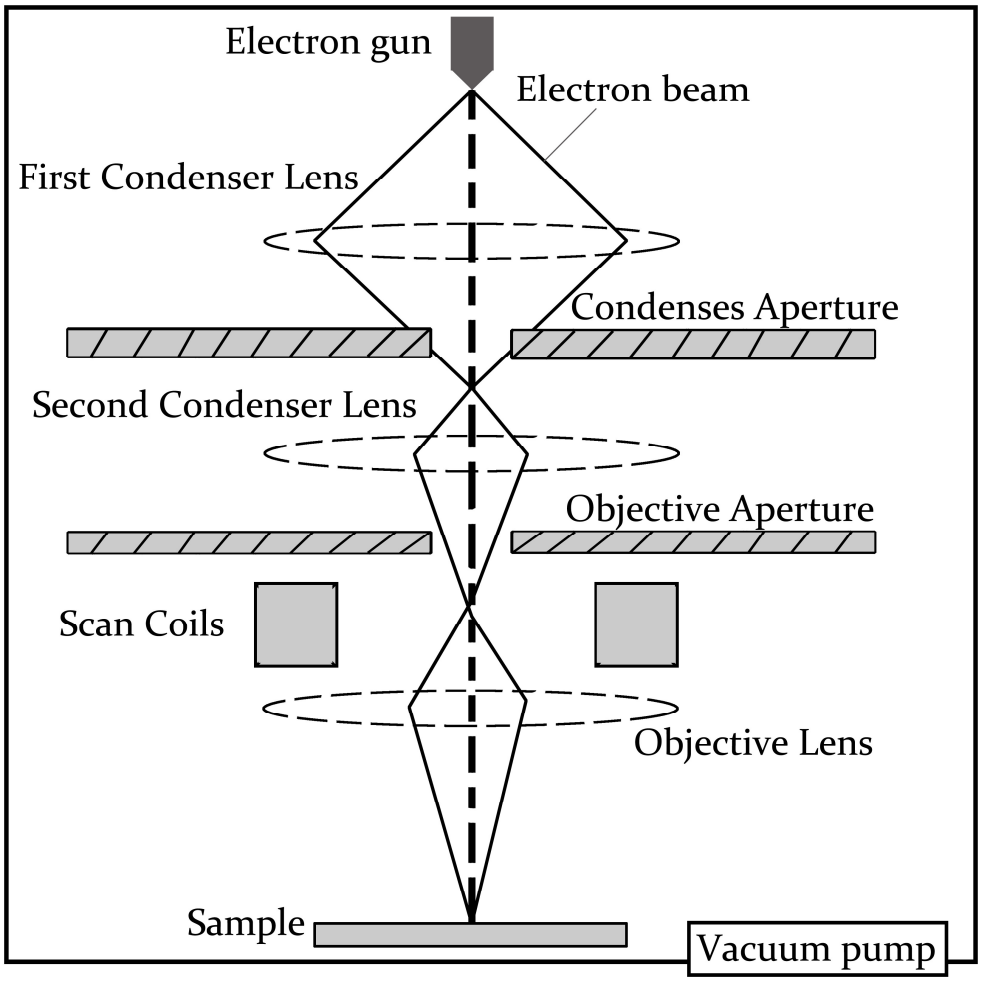

FIGURE 5.3
A schematic diagram of scanning electron microscopy

The SEM generates a beam of electrons in a vacuum system and a resolution can be reached around 1nm in advanced systems such field emission scanning electron microscopy (FESEM). Basically, the principle work of the SEM as shown in figure (5.3) is that the electron beam is generated by electron gun which is made of Tungsten filament, Lab6 (or CeB6) or Field Emission Tip. The beam is collimated by electromagnetic condenser lenses, focused by an objective lens, and scanned across the surface of the sample by electromagnetic deflection coils. The secondary electrons, which are come out from the sample, are collected and detected by producing flashes of light from the electrons. These signals are amplified by a photomultiplier tube. By correlating the sample scan position with the resulting signal, an image can be generated which is noticeably similar to what would be seen through an optical microscope.
In addition, SEM generates a secondary electron i.e. back scattered electron (BSE) that comes out almost 180 degrees from the direction of the beam. These high energy electrons can be used to produce Backscatter imaging. The backscatter electron yield is almost independent of accelerating

voltage, but it is strongly depend on the atomic number of the sample, and therefore can give information about sample compositions [4].

Atomic Force Microscopy (AFM)

Atomic-force microscope (AFM) was discovered by Gerd Binnig and Heinrich Roher in early 1980s at IBM research lab and for this development they got Noble prize in 1986 [6]. AFM was developed just few years after scanning tunneling microscopy (STM) to overcome the limitations of studying non conducting materials. Insulators and semiconductors, as well as electrical conductors, can be studied using AFM.

AFM are useful for application of the physics of solids, thin-film technologies, nanotechnologies; micro and nano-tribology, microelectronics and magnetic record, etc. The AFM is used for imaging matter at a nano-scale, and can be used to manipulate atoms of nanostructure. The AFM can be used in scientific and industrial laboratories. In the AFM system, the image of a surface sample is achieved by scanning a sample by a tip with the curvature radius about few nanometers connected to the cantilever as shown in figure (5.4). A control system map outs the probe position relative the sample surface in each measurement point and the operator can adjust the distance between the tip and sample surface. These data can be employed for further processing, visualization and analysis [7].

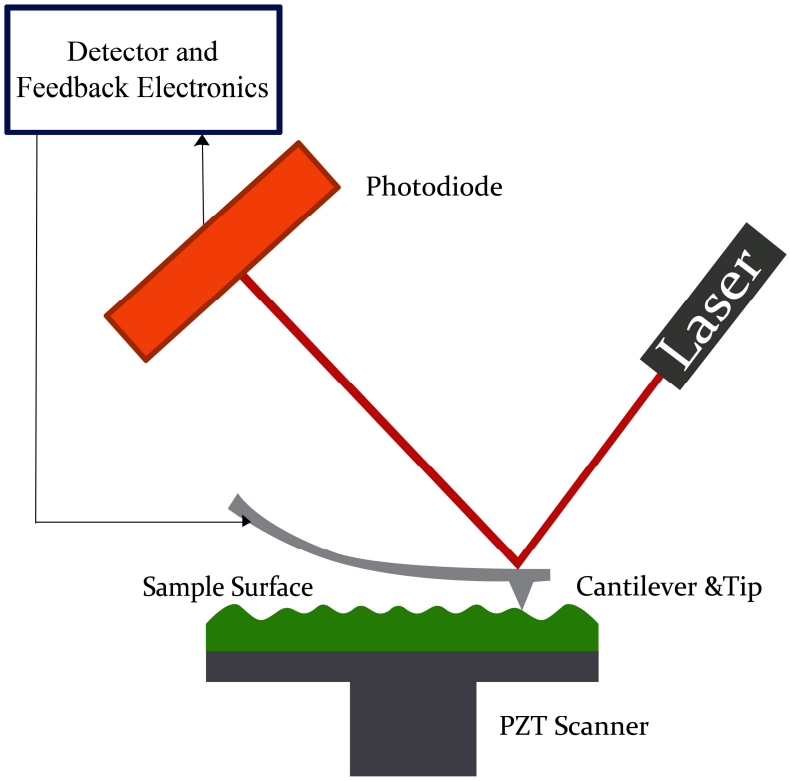

FIGURE 5.4
Block diagram of atomic force microscope (AFM)

Generally, the concept of AFM is like a competition between two forces, when the tip of AFM become closer to sample surface, one is the attractive van der Waals force and the other is an electrostatic repulsive force. It depends on the distance between the tip and the sample. When the tip is very close to the sample, around a few angstroms, the interatomic force is predominantly repulsive because the electron clouds of atoms in the tip and the sample surface are overlapped. This is known as the contact mode. However, in non-contact mode the distance is more than ten angstroms where the interatomic force is attractive due to the long range attractive van der Waals intractions.
The AFM has many advantages in term of instrumental features such as AFM has a laser-beam system for detecting the probe position and torsion. Also, AFM works in two modes operation in static and dynamic modes and by using automation motorized positioning of the measuring head over sample. It is possible that a special kind of arrangement a video system embedded in the measuring head for observing the probe and scanned area on the sample surface. In addition, AFM is easy to connect with host computer via USB port.
Generally, AFM provides the information about only the surface of a sample with any information about the morphology and structure must be obtained by scattering methods such as the SEM technique.

Advanced magnetic materials and techniques

There are many of magnetic materials, but the type of materials which are considered in this section is half metallic ferromagnetic, because its thin films are promising materials for spin-injection/detection into semiconductors such as GaAs due to their high degree spin polarization of their transport current. In a half metallic material the density of states at the Fermi level is finite for just one type of spins and zero for the other. Consequently, the electric current is carried by electrons of one spin orientation. This unique property renders half-metallic ferromagnets as ideal candidates for a huge number of spintronics applications, such as spin field-effect transistors (FET) and many others recently proposed devices.
Perovskite manganites have been an attractive topic under discussion in a huge number of studies owing to their surprising and colossal magnetoresistive (CMR) property [9] along with extraordinary structural, electrical and magnetic properties. The general formula of manganites is $A_{1-x}B_xMnO_3$ where A is a trivalent rare earth cation (such as La, Pr and Nd) and B is a divalent alkaline earth cation (such as Ca, Sr and Ba). Amongst a wide range of such materials, $La_{1-x}Sr_xMnO_3$ (LSMO) illustrates exciting properties such as room temperature ferromagnetism (~ 340K), particularly for optimally hole doping at around x~0.3.
Based on the band theory, the electronic properties of LSMO are almost half-metallic [10, 11], leading to which is known as transport half-metallic behaviour [12]. Even the LSMO has attractive magnetic and electronic properties (such as CMR); it shows very complicated electronic structures in comparison with the normal band theory picture [13]. In particular, the electronic structure is explained by the fighting of double exchange and super-exchange interactions, charge/orbital ordering instabilities and strong coupling with the lattice deformations [14].

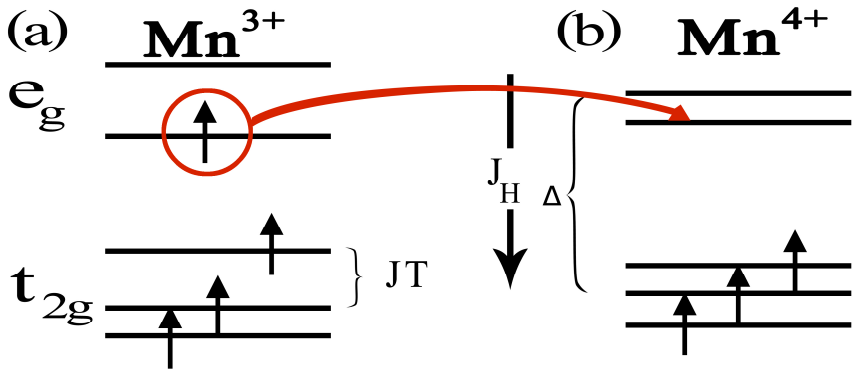

FIGURE 5.5
Schematic of the double exchange mechanism in LSMO

To explain very clearly the electronic and magnetic properties of LSMO, we will use Figure (5.5) which shows the double exchange mechanism in LSMO. First of all, its parent composite $LaMnO_3$ is antiferromagnetic insulator. By replacing the trivalent La cation with a divalent cation (Sr in this case) and based on the electro-neutrality conservation law, the Mn sites have then to suppose a mix between two valences Mn^{+3} and Mn^{+4}. According to Figure (5.5), the exchange energy (J_H ~ 2 eV) is higher than crystal field splitting (Δ ~ 1.5 eV) [15] so that, on a Mn^{3+} site, there are three electrons on the t_{2g} ↑ levels, with one occupying the first level of the e_g ↑ levels. However, in the Mn^{+4} site, the doping leads to the production of a hole in the e_g levels instead of an electron. The double exchange (DE) mechanism, which was proposed by Zener [16], occurs between Mn^{+3} and Mn^{+4} sites across O and leads to an increase in the efficient delocalization of the electron in e_g ↑ at the Mn sites. These exchange interactions need the first and last states to be degenerated in energy. This means that the same spin is referential on each Mn site that is fastened by the three localized electrons in t_{2g}. This spin-conserving mechanism of the electron transport therefore makes sure to extend the ferromagnetism, and the conduction of e_g electrons with spin ↑[13].
The difference in degeneracy between a DE mechanism along a couple of sites, and the revisable interaction, has been discussed for many years ago, as a result of the Jahn–Teller (JT) distortion [16] on the Mn^{+3} site. Recently, this effect can be best understood in terms of metallic manganites because they lead to transport by elastic JT polarons [17]. This cooperative system of transport of e_g↑ levels could be obstructed by several factors such as Anderson localization and differences of the angle in the Mn–O–Mn bond which decreases the e_g bandwidth [17].
We can conclude that the double exchange mechanism (DE) is the interaction between the doping induced carriers and localized spin, namely the strong Hund's role, while the John-Teller (JT) effect is produced by a coupling between charge and lattice. A significant consequence is that below the Curie Temperture (T_c), the ferromagnetic ordering increases with the width of the e_g band. This suppresses the Jahn-Teller effect.
Recently, The LSMO thin film has an effective potential in advanced applications such as magnetic memory storage, sensor and spintronics. Many techniques have been arisen to eliminate the fabrication problems in order to get high quality thin film. PLD technique is one of the best

methods to fabricate such thin films. For example, it can be used to fabricate films at different pressures with a high degree of control even at high pressures.
LSMO thin film which is growing by PLD is a good example to show how we can get high quality thin film. First of all, making the bulk target from very high purity is significant to avoid any contamination. The choice of the type of substrate and preparation play an important role in the quality of the film, and therefore can be affect its properties such as magnetic properties. For example, researcher who is used $SrTiO_3$ (STO) as a substrate for LSMO thin film, has to prepare it very well before growing such as they use wet-etching with buffered hydrofluoric acid, followed by a thermal annealing process. This leads to form a TiO2- eliminated atomically flat top surface on the STO. During the growth, controlling the rate of deposition, substrate temperature, oxygen ambience and other parameters is a key factor to have single crystal thin film as you want for specific applications [18].

Magnetoresistance, magnetoimpedence, spin torque transfer

Magnetoresistance

Controlling the current flow is very important phenomenon for applications. Therefore large effort has been done toward the use of magnetic field to control the resistance in magnetic materials which is called magnetoresistance (MR). The classical treatment of the magnetoresistance effect depends on the strength and relative directions of the magnetic field with respect to the current.
The other advantage of this subject is the new degree of freedom in the current flow known as electron spin which is an intrinsic angular momentum of a particle. In the case of the electron there are two possible states, spin –up and spin-down.

The MR effects in nonmagnetic metals are very small at low field as the large field region has no application interest. The change in resistivity is the same for both magnetic field parallel and transverse to the current direction.
The MR effects in ferromagnetic metals show a variation of about 2% in resistance and anisotropic behavior. The current encounters increasing resistance along the parallel direction and decreasing resistance along the transverse direction relative to the magnetic field direction. The anisotropic magnetoresistance (AMR) behavior appears to be related to the spin orbit coupling, where the magnetization slightly deforms the electron cloud about each nucleus causing the rotations of the closed orbit orientation with respect to the current direction. The resistance would be higher for the current moving parallel to the magnetization direction, as the magnetization rotates the electronic orbits to be perpendicular to the current which increase the cross-section for scattering. While a low resistance for the current move perpendicular to the magnetization direction, as the magnetization rotate the electronic orbits to be parallel to the current which decrease the cross-section for scattering [19, 20].
Colossal magnetoresistance CMR has been found in a structured material consist of a rare-earth element combined with manganese and oxygen doped with Ca or Sr [21]. These materials show an insulator-metal transition depending on the temperature. In the metal regime it becomes ferromagnetic. Magnetic field on the order of 10^4 required to achieve colossal magnetoresistance.
Giant magnetoresistance GMR and tunnel magnetoresistance TMR are unlike the previous MR effects depend on just material properties, they depend on devices Geometry and design using

quantum mechanical effects. Therefore the GMR and TMR have multilayer system consisting of ferromagnetic layers and insulator or semiconductor layers [22].

Magnetoimpedance

A large change of the complex impedance, $Z = R + j\omega L$, where R and L are resistance and inductance, respectively, can be achieved in a soft ferromagnetic conductor only if the system is subject to magnetic field while an alternating current (ac) passes through it. The change of the complex impedance is known as magnetoimpedance MI effect [23]. The magnetoimpedance effect depends on the alternating current (ac) frequency and amplitude, magnetic permeability and the field component on the surface.
The alternating current (ac) frequency classifies the physical factors causing the magnetoimpedance. Therefore, in the frequency range up to several KHz the skin effect is very weak and the impedance of the system while applying the field (Hdc) results mainly from the contribution of inductance (L). However, in the frequency range within 102 ~ 104 KHz and when applying dc magnetic field, the effective magnetic permeability changes strongly causing the variation of the skin depth which initiates the magnetoimpedance. In this range, GM maximum value depends on permeability contribution from domain wall motion and magnetisation rotation simultaneously, as the frequency increases the GM decreases because the contribution becomes only from magnetization rotation. When the frequency is greater than several MHz, the magnetoimpedance is initiated by the gyromagnetic effect and ferromagnetic relaxation [24, 25].

Spin transfer torque

Spin transfer torque can be generated when an electronic current is flowing perpendicular to the plane of the multilayer system. The electronic current passing through the ferromagnetic layer would flow with low resistance if the electrons spin is aligned with the layer magnetization and high resistance if the electrons spin nonaligned with the layer magnetization this proses is used in the GMR. The other possibility is that the electronic current would change its spin direction to be aligned with the magnetization direction, or it may disturb the magnet of the layer by exerting a torque on it. A large current may change the magnetization direction of the layer which give raise to oscillation magnetization or steady state which is also a potential phenomenon to make a new devices [26, 27].

Ultra–thin films and surface effects

Decreasing the size of nanostructured materials leads to dominate the surface effect on most physical properties.
Ultra-thin magnetic films and multilayer in conjunction with the interface and surface effect have unique properties result in significant modification of magnetic properties in comparison to their bulk counterpart [28, 29]. In these structures the electrons are confined in one dimension in the range of nanometer, while they are free to move into the other two directions as in the giant magnetoresistance (GMR). The confinement of electrons introduces new fundamental phenomena such as quantum tunneling in tunneling magnetoresistance (TMR). The confinement and tunneling are known as quantum size effects, which in metals require the preparation of samples with high skill controlled thicknesses in the order of one atomic layer because of the density of state

wavelength in the range of the Fermi wavelength [30]. The high density of electrons create strong efficient screening defect of the columbic potential which let the electron feel the boundary effect only in the last one or two atomic layer away from an interface or a surface. Therefore, in magnetic material the layer thickness has to go down to few nm to be able to get the quantum size effect in the devices such as TMR, GMR and AMR, in general the Magneto-electronics or Spintronics devices which are the key areas of Information Technology. According to Koksharov, [31] finite size effects are defined as follows: "in the view of condensed matter physics, finite size effects are originated by the cut off of characteristic length, resulting from the geometric limitation of the particle. In certain sense, surface effects can be considered as a sort of finite size effects since the surface influence is most significant in smallest nanoparticles and should vanish for large particles."
Interface and finite size effects can be seen not only in the quantizing of the electron wave function but more significantly in the transition metal oxides material specifically where the strain has a strong influence on the electrical, optical, and magnetic properties [32]. The fascinating properties initiated by the interactions between lattice, spin, charge and orbital degrees of the transition metal oxides [33].
Recent advances in growth of ultra-thin films and low dimensional structures show the opportunity of putting on the surface large and non-hydrostatic stress taking advantage from the smaller number of structural defects in the low dimensional systems [34]. Biaxial strain of several percent can be enforced on the ultrathin film by the substrate through the lattice mismatch. Biaxial strain can be used to control the transition temperature in high-TC superconductors [35], ferroelectric materials [36] and spontaneous polarization in ferroelectrics [37,38].

Multi-layered films and superlattice structures, interface effects

Magneto-resistance is basically the change of resistivity with the application of a magnetic field, which is defined as

$$\frac{\Delta\rho}{\rho H} = \frac{\rho(H)-\rho(0)}{\rho(H)} \qquad (1.1)$$

Where $\rho(H)$ is the resistance under the magnetic field and $\rho(0)$ is the resistance without the magnetic field. When this change is very large then it is called colossal magneto-resistance (CMR). This is the most interesting property for magnetic applications.
The most common types of multi-layered films are Giant magnetoresistance (GMR) and Tunneling magnetoresistance (TMR). The GMR phenomenon was discovered by Peter Grünberg and Albert Fert and they awarded the Nobel Prize in Physics in 2007 [39]. The significant difference between GMR and TMR is the presence of the sandwich layer between the ferromagnetic layers, where in GMR model the layer is conductor layer, but insulator layer is used in TMR type.
The resistance of GMR can be simply explained by using the figure (5.6). The magnetic configuration for GMR model FM/NM/FM (ferromagnetic/non-mag-netic/ferromagnetic) multilayer is plotted to understand the mechanism very well. Without applying magnetic field, the magnetic layers are antiparallel (the top one), whereas in presence of magnetic field the magnetic layers take the same magnetization direction (the bottom one). The current consist of two types; spin up and spin down current. Each one has different resistance within the ferromagnetic layer and also the resistance at FM/NM interface. Inside the Non Magnetic layer the both spins will face the same resistance. However, this resistance is a quite small in comparison with those in the FM layers and

FM/NM interfaces and therefore it can be ignored [39].

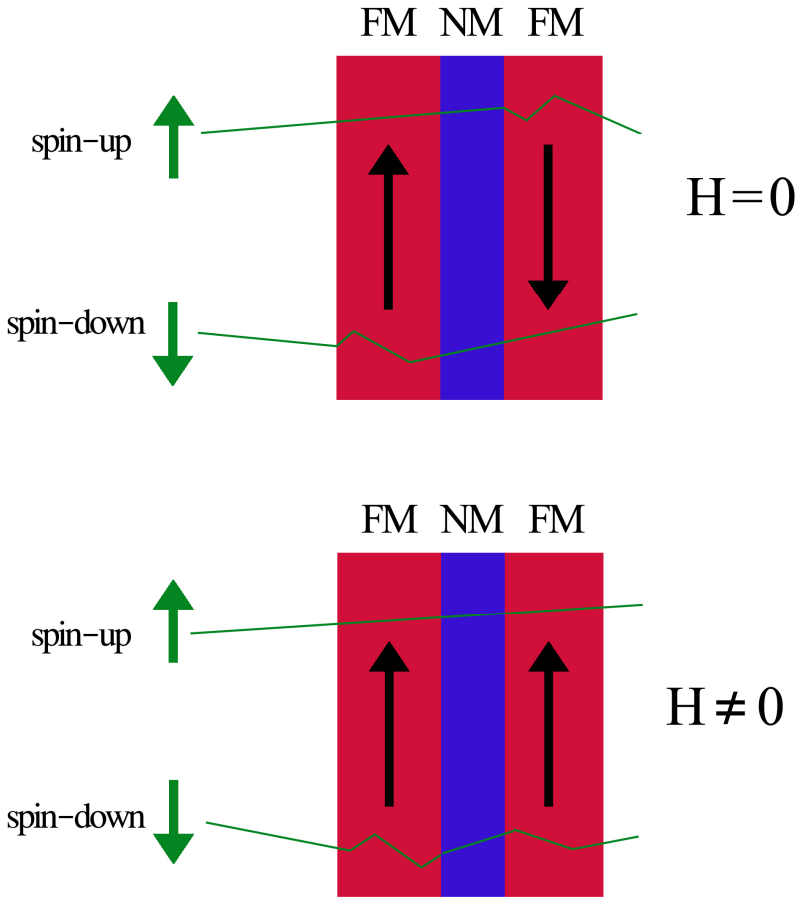

FIGURE 5.6
The diagram of Giant magnetoresistance (GMR)

The same principle can be applied to TMR which based on the tunneling effect in quantum mechanics. It is important to note that the thickness of insulating layer is very critical and must be within few atomic layers to allow such phenomena to happen.
Alternating by making layers of (FM/NM/FM/NM/FM……./FM) is known as superlattice. Some scientists use this method to improve the magnetoresistance, but they may face the interface problem.
In the rest of this section, I will consider a practical example to make the picture is very clear about the interface problem between two materials which are in our case La0.7Sr0.3MnO3 (LSMO) and SrTiO (STO). The mismatch between the LSMO and the substrate (STO) is a very significant factor, because it can result from a tensile strain in the film. This can affect two factors that determine the co-operative interaction and therefore the transport or the magnetic properties: (i) the amplified Jahn–Teller distortion results in a localization of electrons; (ii) the expansion or reduction of the

Mn–O–Mn bond-length results in a great decrease or increase of the electronic hopping amplitude. Reducing the film thickness can lead to a high tensile strain in the film. As a result, lattice distortion decreases the hopping amplitude, which makes various interactions in competing, resulting in electronic phase separation. Experimentally, it has been found that the in-plane tensile strain likes the A-type antiferromagnetic ordering and the in-plane compressive strain likes the C-type antiferromagnetic ordering [40, 41]. The bi-axial strain favours the antiferromagnetic charge-ordered, whilst the inhumongous distribution of the strain enhances the phase coexistence. Even though the lattice mismatch between LSMO and STO substrate is just −0.5%, there has been a distribution of strain. This strain is supposed to be quite relaxed on the top of a large grain, but to be highly strained in the site which is closed to the substrate. The building of the ferromagnetic metallic regions at the cost of the charge-ordered insulating areas on the application of the magnetic field, results in an enormous negative MR in LSMO/STO (10 nm) film. Another popular substrate for LSMO is $LaAlO_3$ (LAO). The lattice mismatch between the LSMO and $LaAlO_3$ (LAO) is around +2% which leads to bi-axial compressive stress. The lattice mismatch of LSMO/LAO is higher than that of LSMO/STO. This suggests that the indication of phase separation is supposed be more obvious in LSMO/LAO. This makes choosing the appropriate substrate for fabricating thin film extremely crucial, since a good match between the manganite and the substrate is required in order to create a high quality film [42].

Exchange bias

The exchange bias has been discovered in 1956 by Meiklejohn and Bean [43], this complex phenomena required specific conditions to be observed. Cooling the Ferromagnatic (FM) – antiferromagnetic (AFM) interface system while it is exposed to low magnetic field from temperature T_1 above Neel temperature T_N of AMF but less than Cure temperature T_C of FM ($T_C>T_1>T_N$) to temperature T_2 (in the order of 10 K) less then T_N ($T_2<T_N$) would lead to the exchange bias (anisotropy) phenomena. Since then this phenomenon has been observed in the systems of AFM/FM interface for different material and different structures searching for a better control over the interface and more reliable for devices applications [44-49].

In the AFM/FM interface system under a field cooling treatment, the hysteresis loop would move relatively, known as exchange bias H_E, in direction opposite to the cooling field along the field axis Figure (5.7). An increase of coercive field H_C would associate the exchange bias phenomena. The AFM material responsibility of the two phenomena is confirmed by their disappearance as the temperature of AFM approach the T_N [44, 50]. The other phonomena associated with exchange bias is unidirectional anisotropy which represents the magnetization direction.

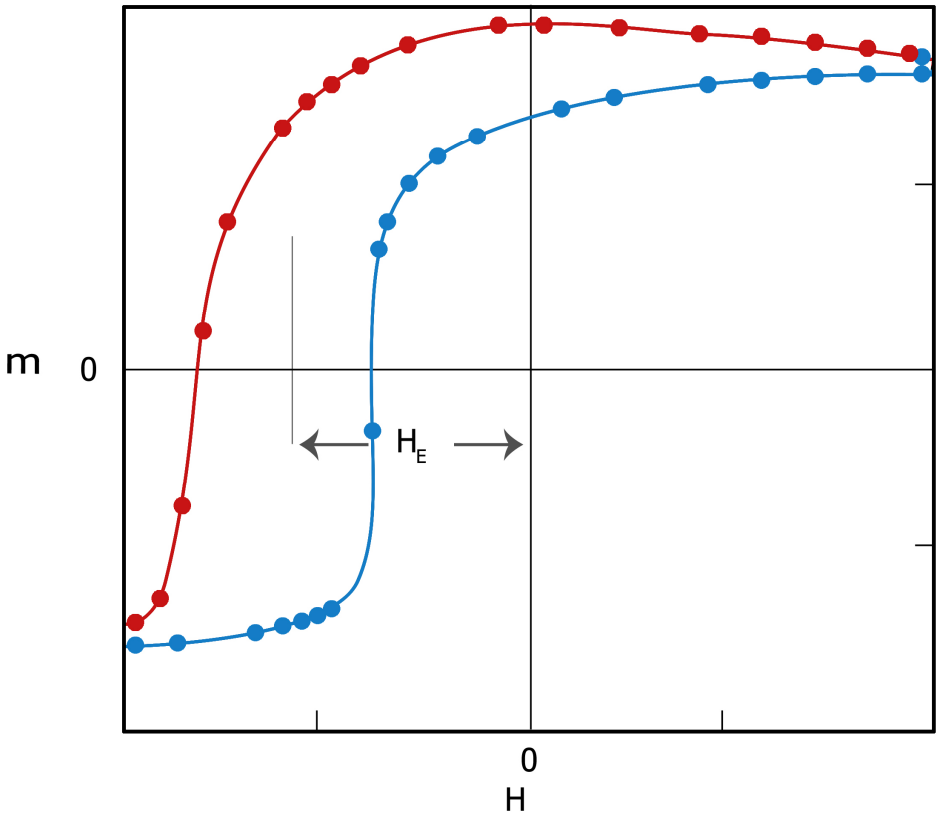

FIGURE 5.7
The hysteresis loop, where H_E is the exchange bias

The simple picture to make these phenomena qualitatively clear is by considering layer of AFM and another of FM with interface, if both layers at temperature T_1 are subject to magnetic field then the spins in the FM layer align with magnetic field while the AFM spins stay in random order. When the system is cooled down from T_1 to T_2 ($T_2<T_N$) the AFM spins start to get in a specific order, where as spins in the plan next to the FM would take their alignment and the next plan spins would be in opposite directions and so on in order to keep the total magnetization in the AFM layer equal to zero. When the magnetic field is reversed, the AFM spins would not be changed because of the large anisotropy while the FM spins would start to rotate, however the first spins plan of the AFM at the interface would exert a microscopic torque on the FM spins. Therefore, it is necessary to have a larger field to make FM spins fully align with the magnetic field, for this reason the FM spin have unidirectional anisotropy. When the magnetic field is changed to its original direction the FM spins would rotate with lower field as this time the first plan spin in the AFM acts as an internal torque supporting the FM spins to rotates back to the first alignment. This is equivalent to biasing field causing the hysteresis loop to move along the magnetic field known as exchange bias.

Magnetic nanoparticles and nanostructures

The magnetic nanostructures show unusual properties in comparison with those of microstructures. Indeed, particularly the magnetic properties are strongly correlated to the enhanced presence of surface, interfaces or grain boundaries, according to the nature of the nanostructures. Magnetic nanoparticles and nanostructures are playing an important role in many promising applications such as drug delivery. Although felicitous methods of preparation such materials have been developed, the stability of the particles under a specific conditions is shaky. However, in most of applications, results shows a great performance below the critical size of nanoparticles (below 100nm) when the particles become single magnetic domain. In this range and when the temperature is above the blocking temperature. Nonetheless, this feature is instable due to the highly chemical activity and the oxidation in air. For many applications, it has been important to develop protection strategies to make the magnetic nanoparticles chemically stable. An example of these strategies of protection is coating with organic species such as polymers or with an inorganic species such as carbon. These functionalized nanoparticles are very hopeful in bioseparation, catalysis, and biolabeling. It is significant to focus on the two special features of magnetic materials at nanoscle, namely finite size effects and surface effect [51,52].

Finite size effects

The most studies of finite size effects in nanoparticles are on the single domain limit and the superparamagnatic limit. For any magnetic material, there are walls separate the uniform magnetization for the structure. The magetostatic energy (ΔEms) drives the formation of this wall. ΔEms is proportionally dependent on the volume of the material. The domain wall is proportionally dependent on the interfacial area between domains. Reducing the material size will cost a lot of energy to create a domain wall more than supporting the external magetostatic energy of the single domain [51].

Surface effect

The large portion of atoms in the nanomaterials is located on the surface by decreasing the particle size. Therefore, the surface and the interface effect became more important. This kind of effects may lead to decrease the magnetization of the small particle. In such cases, coating the surface is the way to protect the magnetization [53].

Synthesis and Protection of Magnetic nanomaterials

Verities of compositions and phases have been synthesized the magnetic nanoparticles such as Fe3O4. Researchers have reported so many ways of synthesis such as Thermal Decompositions, Co-Precipitation, Microemulsion and Hydrothermal synthesis. By hydrothermal synthesis, a wide range of nanostructure material may be composed. This method is based on a general phase of liquid and solid solution phases present during the synthesis. Despite the method is not perfectly clear yet, the multicomponet way looks powerful in directing the formation of desired material. Whereas there are numerous methods of synthesis magnetic nanoparticles, there is an issue with the stability of this particle with time. Thus, protection ways have emerged like coating with specific material. Coating MNPs can be classified into two main groups. Coating with organic shells, including surfactant and polymers. Generally, electrostatic or static repulsion could be employed

for divide nanoparticles and remain them in a stable colloidal state [54], or coating with inorganic components, including carbon, precious metals and silica which prevent the direct contact of the magnetic core with additional agents linked to the silica surface to avoid the interaction[52].

Magnetic microscopy, imaging and characterization

In this section, various methods to measure the magnetic properties will be discussed. The magnetic force microscopy (MFM) is very useful technique for imaging and shows the magnetic domains in the samples. In addition, superconducting quantum interference device (SQUID magnetometer) gives the information about the magnetization even it is very low signal because it is very sensitive method. Finally, the magneto-optics Kerr effect (MOKE) method is an optical technique to study the magnetic properties.

Magnetic Force Microscopy (MFM)

Based on the information of normal AFM which was discussed at the beginning of this chapter, we are focusing on a special mode of operation of the AFM which is Magnetic force microscopy (MFM).

In this case, the system uses a magnetic tip which is usually is made of nanomagnetic materials. Coating a normal tip with magnetic materials can be used as well. The tip radius of curvature is around few nanometers. Sharper tip radius allows for higher resolution topological scan, which leads a more precise height profile for the tip to follow [55,56].

MFM is a scanning probe microscope technique, and it is a powerful technique for imaging magnetic domains. By measuring the magnetic interaction between a sample surface and a tip allows us to map the spatial distribution of magnetism as shown in figure (5.8). The principle work of such measurements is that the AFM contain a flexible cantilever hanged from one side where another side is attached with a small magnetic tip. During the measurement, when the tip closes to surface of the magnetic material, it interacts with the stray magnetic field which is coming from the magnetic sample. This interaction can be measured by detecting the cantilever motion with a sensitive optical deflection detector and therefore to measure the force gradient [57].

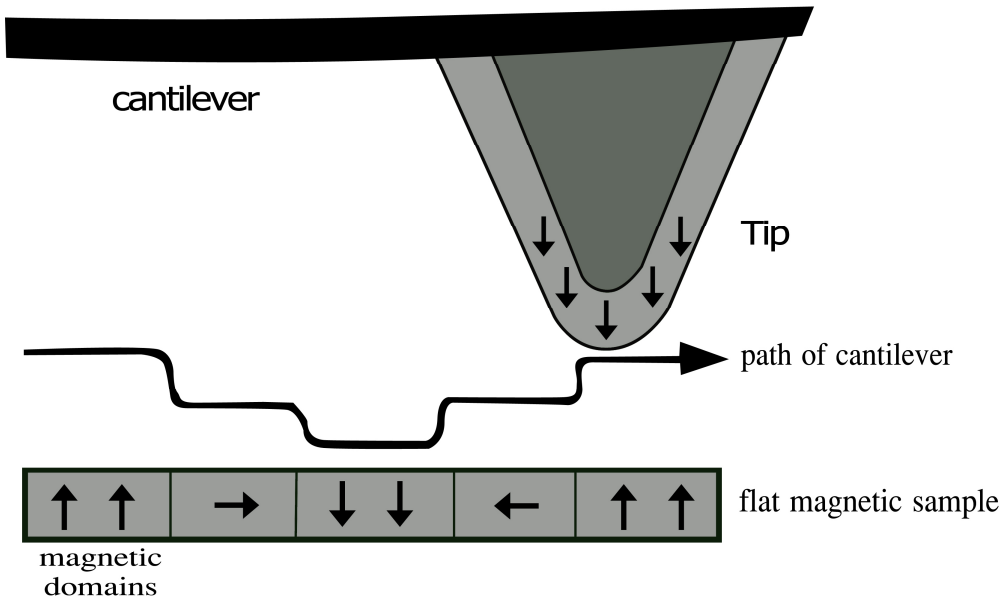

FIGURE 5.8
The magnetic interaction between a sample and a tip

Superconducting Quantum Interference Device (SQUID magnetometer)

The superconducting quantum interface device (SQUID) is very sensitive to magnetization, even though it is very small. It consists essentially of two parts: a superconducting ring and a "weak-link". The weak-link or Josephson junction, is a very thin resistive area in the superconducting ring in a SQUID. It is important to note that the SQUID magnetometer can have a wide range of applications such as biomagnetism and material property measurements [58-60].
The experimental set-up for measuring magnetization by using a SQUID magnetometer is not complicated. A sample on a substrate, which is usually around a millimetre in size, is mounted on uniform plastic straw with or without a gelatine capsule, depending on its size. After this, the straw is stuck to a sample-holder of SQUID magnetometer which is located on the top of it. An air-lock should be closed while sticking the sample to the holder to avoid the sample chamber becoming contaminated by atmospheric air.
Before starting a scan, the sample must be centred, either manually or automatically. The centring the sample means putting it into the centre of the field-sensing coils. A full test of 2cm is the scan sequence used for the measurement. In a scan, the sample is staged through a number of second-order gradiometer field-sensing coils. This contains of couple of sets of oppositely wound coils that provide more precise measurements by being insensitive to uniform fields and uniform field gradients. The sample produces a field which, in sequence, leads to a super-current in the coils and thus a magnetic flux through the ring. Because of these, measurements increase as a function of the field of the magnetisation of the sample and can be obtained by applying an externally magnetic field. The magnetization results of a sample are typically made of contributions from the film and the substrate. The ferromagnetic contribution from the film is saturated at a low field,

whereas the diamagnetic contribution from the substrate is indicated linear dependant at high field.

Magneto-Optics technique

The magneto-optics (MO) effect is the change of intensity or polarization caused by magnetization. In other words, it is the change of linear polarization to elliptically polarized light, with the rotation of the principal axis which leads to a difference in the optical response between left and right circularly polarised (LCP and RCP) [61,62].
Assume that we have a medium with thickness L, and with light moving through it. This medium will have a refractive index $\tilde{n}$, which is composed of two parts, namely real and imaginary parts

$$\tilde{n} = n_0 + ik \tag{1.2}$$

Now, we write the wave vector of the light *(q*) in expressions of the refractive index $\tilde{n}$ and its frequency, *ω*. This step can be employed to calculate the electric vector of the light, *E*, both going into and out of the medium.

$$q = \frac{\omega\tilde{n}}{c} \tag{1.3}$$

$$\begin{aligned} E_{out}\exp(i\omega t) &= E_{in}\exp(iLq)\exp(i\omega t) \\ &= E_{in}\exp\left(\frac{iL\omega\tilde{n}}{c}\right)\exp(i\omega t) \\ &= E_{in}\left(\exp\left(\frac{iL\omega n_0}{c}\right)\exp\left(-\frac{L\omega k}{c}\right)\right)\exp(i\omega t) \end{aligned} \tag{1.4}$$

If the two parts LCP and RCP are similar, the light is linearly polarised as shown in Figure (5.9.a). It can be degenerated to these two situations and moved through a magnetic material. Now, we can rewrite equation (1) as

$$\tilde{n}_{\pm} = n_{0\pm} + ik_{\pm} \tag{1.5}$$

where the positive term corresponds to the RCP light and the negative one corresponds to the LCP light [61, 62].

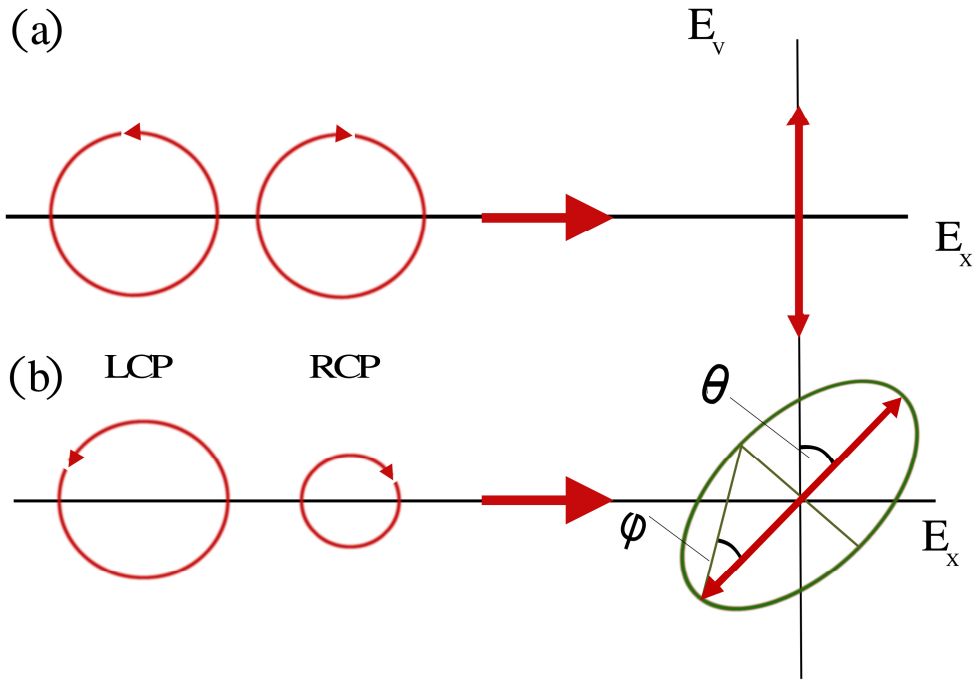

FIGURE 5.9
(a) linear light has similar LCP and RCP. (b) If the light incidents on a sample with a magnetic field, the light will be elliptically polarised and rotated with angle. [28]

An MO effect can occur if the refractive indices of LCP and RCP are not the same, ($\tilde{n}_+ \neq \tilde{n}_-$). This leads to a modification in phase and amplitude of each LCP and RCP light, as shown in Figure (5.9.b). This then results in elliptically polarised light with a rotation angle ϑ. Electric dipole transitions are responsible for the refractive index and the absorption of light in a solid. Circularly polarised transitions will take place between magnetically quantized electronic states when Δm_j = ±1. The weak spin-orbit coupling can occur when the allowed selection rules are $\Delta m_s = 0$ and $\Delta m_l = \pm 1$ [61].

In the transmission case, the rotation and ellipticity of circularly polarised light leads to the magneto-optics effects of both the Faraday Effect and magnetic circular dichorism (MCD) [63]. Basically, the Faraday Effect measures the difference between LCP and RCP light in refractive indices. The Faraday Effect measurement can be very significant as it is finite in spectral regions where the crystal is not absorbing. However, it can also be very complicated for thin magnetic films due to a large Faraday Effect from the substrate and interference effects in the thin film [61].
The MCD is the difference in the intensity for left and right circularly polarised light at a frequency ω. It gives the information about the magnetic state of the two energy levels in the transition. Moreover, an MCD at the band edge indicates that either the valance or the conduction band or both is spin split, so an MCD at the band edge is a test for polarised carriers. Furthermore, it is one of the very few methods for getting information about the polarisation of the conduction bands without having to extract the carriers through a surface. This makes the MO effects very sensitive

to the magnetic electron states such as the 3*d* states of Mn ions in manganites. Because it is only reliant upon transitions at ω, it is only non-zero if the crystal is absorbing. This makes the MCD very useful in defining the nature of magnetic states and any electronic transition included [64].

Conclusion

Nanomagnetism covers a wide range of the research area of advanced technology. It has promising applications such as data storage, magnetic sensor and drug delivery. Our aim of this chapter is to show that the well known concepts of nanomagnetism and magnetic properties at nano level could serve as a good starting point to explore nanomagnetism and its phenomena. We started with a brief discussion of the synthesis and the characterization of nanostructured materials including their principles and methods. General critical phenomena were considered through this chapter such as ultra–thin films, surface effects and interface effects. Also, special magnetic features were discussed in details such as magnetoresistance, magnetoimpedence and Exchange bias. LSMO magnetic thin film, which is promising material due to spin polarization, was used as an example to clarify some of the concepts. The protection methods of magnetic nanoparticles were taken into account as well. Finally, the imaging and characterization of magnetic materials were discussed and explained in details.

Acknowledgements

I would like to thank my condensed matter group at national center for applied physics at King Abdulaziz City for science and Technology (KACST). I would like to show my deepest and special thanks to Dr. Omar Al-Dossary who has giving me very useful advices while I am writing this chapter. I am also extremely grateful to Mr. Ahmed AlQarni for his help. Also, I would like to extend my appreciation to Dr.Mohammad A. Alduraibiand Mr. Mr. Abdulrhman Hiazaa.

References

1. Chrisey D B and Hubler G K (ed). Pulsed Laser Deposition of Thin Films. New York: Wiley-VCH); 1994.
2. Dagotto A, Hotta T and. Moreo A 2001 Phys. Rep. 344 1.
3. P.J. Kelly, R.D. Arnell. Vacuum 56 (2000) 159-172.
4. Robert W. Kelsall, Ian W. Hamley and Mark Geoghegan. Nanoscale Science and Technology. John Wiley & Sons Ltd; 2005.
5. P. J. Goodhew and F. J. Humphreys. Electron Microscopy and Analysis, 2rd Ed. Taylor and Francis, 1988.
6. Binnig, G., Quate, C. F. & Gerber, C. Atomic force microscope. *Phys. Rev. Lett.* **56**, 930–933 (1986).
7. Pedro J. de Pablo. Single Molecule Analysis Methods in Molecular Biology, Introduction to Atomic Force Microscopy, Springer, Volume 783, 2011, pp 197-212.
8. Gary M. McClelland, Ragnar Erlandsson and Shirley Chiang. Review of Progress in Quantitative Nondestructive Evaluation, Atomic Force Microscopy: General Principles and a New Implementation. Springer, Volume 6 A, 1987, pp 1307-1314.
9. W.E.Picket, D.J. Singh, *JMMM* **172**, 237 (1997).
10. E.A. Livesay *et al*., *J. Phys. Cond. Matt*. **11**, L2711 (1999).
11. B. Nadgorny *et al.*, *Phys.Rev. B* **63**, 184433 (2001).
12. Y. Tokura, Y. Tamioka, *JMMM* **200**, 1 (1999).
13. M. Bowen et al., *J. Phys.: Condens. Matter* **19**, 315208 (2007).
14. Coey M et al., *Adv. Phys.* **48** 167 (1999).
15. Zener C, *Phys. Rev.* **82** 403 (1951).
16. Jahn A and Teller E, *Proc. R. Soc. A* **161** 220 (1937).
17. Millis A, *Nature* **392** 147 (1998).
18. S. Jin et al., *Science* **264,** 413-415 (1994).
19. C. Kittel,QuantumTheoryofSolids,JohnWiley& Sons,Inc., p239 (1963).
20. Janice NickelMagnetoresistance OverviewComputer Peripherals LaboratoryHPL-95-60June, 1995.
21. S. Jin1, T. H. Tiefel, M. McCormack, R. A. Fastnacht, R. Ramesh, L. H. Chen, Science V264, p413 (1994).
22. M. N. Baibich, J. M. Broto, A. Fert, F. Nguyen Van Dau, F. Petroff, P. Etienne, G. Creuzet, A. Friederich, and J. ChazelasPhys. Rev. Lett. 61, 2472, (1988).
23. Panina LV, Mohri K. ApplPhysLett 1994;65:1189–91.
24. Panina LV, Mohri K, Uchiyama T, Noda M. IEEE Trans Magn 1995;31:1249–60.
25. M.-H. Phan, H.-X. Peng / Progress in Materials Science 53 (2008) 323–420
26. L. Berger,J. Appl. Phys. 49, 2156 (1978); 50, 2137 (1979).
27. Keith Gilmore, Ion Garate, Allan H. MacDonald, and M. D. Stiles.PHYS. REV. B 84, 224412 (2011).
28. Gradmann, U.; Elmers, H. J.; Przybylski, M.: Magnetic Properties of Ultra-thin Films. In: J. de Physique 49, 1988, Nr. 12, S. C8-1665 - C8-1669.
29. F. Kurth, M. Weisheit, K. Leistner, T. Gemming, B. Holzapfel, L. Schultz, S. Faehler. Physical Review B 82 (2010) Nr. 18, S. 184404/1-8
30. P. Brunoin ``Synchrotron Radiation and Magnetism'', edited by É. Beaurepaire, B .Carrière, and J.-P. Kappler, pp. 211-243, Les Éditions de Physique, Les Ulis(1997)

31. Y. A. Koksharov, in Magnetic Nanoparticles, edited by S. P.GubinWiley VCH, Weinheim, 2009, Chap. 6, p. 205.
32. JinboCaoa and Junqiao Wu . Materials Science and Engineering R 71 (2011) 35–52
33. N.A. Spaldin, M. Fiebig, Science 309 (2005) 391–392.
34. A.K. Goswami, L.E. Cross, Phys. Rev. 171 (1968) 549.
35. I. Bozovic, G. Logvenov, I. Belca, B. Narimbetov, I. Sveklo, Phys. Rev. Lett. 89 (2002) 107001.
36. J.H. Haeni, P. Irvin, W. Chang, R. Uecker, P. Reiche, Y.L. Li, S. Choudhury, W. Tian, M.E. Hawley, B. Craigo, A.K. Tagantsev, X.Q. Pan, S.K. Streiffer, L.Q. Chen, S.W.Kirchoefer, J. Levy, D.G. Schlom, Nature 430 (2004) 758–761.
37. K.J. Choi, M. Biegalski, Y.L. Li, A. Sharan, J. Schubert, R. Uecker, P. Reiche, Y.B. Chen,X.Q. Pan, V. Gopalan, L.-Q. Chen, D.G. Schlom, C.B. Eom, Science 306 (2004) 1005– 1009.
38. J. Wang, J.B. Neaton, H. Zheng, V. Nagarajan, S.B. Ogale, B. Liu, D. Viehland, V.Vaithyanathan, D.G. Schlom, U.V. Waghmare, N.A. Spaldin, K.M. Rabe, M. Wuttig, R. Ramesh, Science 299 (2003) 1719–1722.
39. Albert Fert. Nobel Lecture: Origin, development, and future of spintronics. Rev. Mod. Phys., Vol. 80, No. 4, October–December 2008.
40. Tebano A et al., Phys. Rev. B 74 245116 (2006).
41. Aruta C et al., Phys. Rev. B 73 235121(2006).
42. Soumik Mukhopadhyay et al., J. Phys.: Condens. Matter 21 026017 (2009).
43. W.H. Meiklejohn, C.P. Bean, Phys. Rev. 102 (1956) 1413.
44. A. Yelon, in: M.H. Francombe, R.W. Hoяman(Eds.), Physics of Thin Films, vol. 6, Academic Press, NewYork, 1971, p. 205.
45. N.H. March, P. Lambin, F. Herman, J. Magn.Magn. Mater.44 (1984) 1.
46. T.J. Moran, J.M. Gallego, I.K. Schuller, J. Appl. Phys. 78(1995) 1887.
47. W.H. Meiklejohn, C.P. Bean, Phys. Rev. 105 (1957) 904.
48. R. Jungblut, R. Coehoorn, M.T. Johnson, J. aan deStegge, A. Reinders, J. Appl. Phys. 75 (1994) 6659.
49. P.J. van der Zaag, R.M. Wolf, A.R. Ball, C. Bordel, L.F.Feiner, R. Jungblut, J. Magn. Magn.Mater.148 (1995)346.
50. J. Nogue&s, I.K. Schuller/ Journal of Magnetism and Magnetic Materials 192 (1999) 203-232.
51. F. Sch_th et al. Angew. Chem. Int. Ed. 46, 2007 1222 – 1244.
52. Gao et al. Angew. Accounts Of Chemical Research. 42, 8,(2009) 1097-1107.
53. X. Batlle, A. Labarta, J. Phys. D 2002, 35, R15.
54. S. S. Papell, US Patent 3215572, 1965.
55. Porthun S., Abelmann L., & Lodder C. Magnetic force microscopy of thin film media for high density magnetic recording, Journal of Magnetism and Magnetic Materials, Vol. 182, No. 1-2,(1998) pp. 238-273.
56. Hartmann U. Magnetic force microscopy, Annual Review of Materials Research, Vol. 29,(1999) pp. 53-87.
57. Alex Hubert and Rudolf Schäfer. Magnetic Domain the Analysis of Magnetic Microstructures. Springer, (1998).
58. Wikswo, J.P., Jr. Applied Superconductivity, IEEE Transactions on, 5, 2, 74-120 (1995).
59. J.C. Gallop and B.W. Petley, Journ. of Phys. E 9, pp 417 (1976).
60. J. Clarke, Superconductor Applications: SQUID and Machines, ed. B.B. Schwartz and S. Foner, Plenum Press, New York (1977).

61. Anthony Behan, 2008, Characterisation of Doped ZnO Thin Films for Spintronic Applications, PhD thesis, University of Sheffield, UK.
62. Sukhorukov, Y., et al., Technical Physics, 46, 6 (2001).
63. F. J. Kahn and P. S. Pershan, Phys. Rev. 186, 3 (1969).
64. T. K. Nath, et al., J. Appl. Phys, 105, 07D709 (2009).